Transient cavitation in high-quality-factor resonators at high static pressures

D. Felipe Gaitan,[a] Ross A. Tessien, Robert A. Hiller, Joel Gutierrez, Corey Scott, Henry Tardif, and Brant Callahan
Impulse Devices, Inc., 13366 Grass Valley Avenue, Unit H, Grass Valley, California 95945

Thomas J. Matula and Lawrence A. Crum
Applied Physics Laboratory, University of Washington, Seattle, Washington 98105

R. Glynn Holt
Boston University, Boston, Massachusetts 02215

Charles C. Church and Jason L. Raymond
National Center for Physical Acoustics, University of Mississippi, University, MS 38677

(Received 3 November 2008; revised 9 March 2010; accepted 10 March 2010)

It is well known that cavitation collapse can generate intense concentrations of mechanical energy, sufficient to erode even the hardest metals and to generate light emissions visible to the naked eye [sonoluminescence (SL)]. Considerable attention has been devoted to the phenomenon of "single bubble sonoluminescence" (SBSL) in which a single stable cavitation bubble radiates light flashes each and every acoustic cycle. Most of these studies involve acoustic resonators in which the ambient pressure is near 0.1 MPa (1 bar), and with acoustic driving pressures on the order of 0.1 MPa. This study describes a high-quality factor, spherical resonator capable of achieving acoustic cavitation at ambient pressures in excess of 30 MPa (300 bars). This system generates bursts of violent inertial cavitation events lasting only a few milliseconds (hundreds of acoustic cycles), in contrast with the repetitive cavitation events (lasting several minutes) observed in SBSL; accordingly, these events are described as "inertial transient cavitation." Cavitation observed in this high pressure resonator is characterized by flashes of light with intensities up to 1000 times brighter than SBSL flashes, as well as spherical shock waves with amplitudes exceeding 30 MPa at the resonator wall. Both SL and shock amplitudes increase with static pressure.
 [DOI: 10.1121/1.3377062]

PACS number(s): 43.35.Ei, 43.35.Hl [ADP] Pages: 3456–3465

I. INTRODUCTION

Sonoluminescence (SL) has attracted considerable attention from researchers because it represents an energy concentration of several orders of magnitude[1] and also provides an indicator of the violence of cavitation collapse. Cavitation collapse itself has been suggested as a potential mechanism for the induction of thermonuclear fusion,[2,3] although no credible evidence has yet been presented to support such claims.[4–6] Nevertheless, the region within a collapsing cavitation bubble is one of extreme conditions and represents a fertile environment for the study of exciting new physics. For example, inside the cavity at the moment of collapse, the gas and/or vapor have been reported to reach temperatures and pressures on the order of 10^4-10^5 K and 10^4 MPa (100 kbars), respectively.[7–14] These conditions are sufficient to cause the emission of photons with reported energies between ~1 and 50 eV in different liquids.[15–19] For comparison, the surface of the sun is about 0.7 eV and the pressure at the deepest depth in the ocean is about 1.1 kbars.

In this study, we sought to develop a system that would generate the most violent cavitation ever produced, mainly by constructing an apparatus that could initiate cavitation even at static (ambient) pressures (P_{stat}) of several hundred atmospheres. In order to do this, it was necessary to construct a high-quality-factor (Q), spherical resonator that could produce rarefaction pressures in excess of the applied ambient pressure; i.e., greater than several hundred bars. It was determined that in order to enable cavitation at high ambient pressures, it was necessary for the resonator to have a high Q. Furthermore, the high Q values also cause the cavitation events to have short lifetimes (~1–5 ms). We borrow a term from cavitation history, viz., "inertial transient" cavitation to describe this phenomenon because we observe inertial cavitation that lasts for only a few hundred cycles, unlike single bubble SL (SBSL) which is a form of inertial cavitation that can be sustained indefinitely.

II. APPARATUS

A photograph of a typical stainless steel (SS) resonator developed for this study is shown in Fig. 1. In this system, a Tonpilz-type lead zirconate titanate (PZT) piezoelectric driver (i.e., transducer) was used to excite a standing wave sound field in the liquid at frequencies corresponding to the

[a]Author to whom correspondence should be addressed. Electronic mail: gaitan@impulsedevices.com

FIG. 1. (Color online) Stainless steel (SS) spherical resonator (24.1 cm OD and 20.3 cm ID), with Tonpilz-type horn transducer (top-left), PZT surface transducer (pill) attached near the equator (center with cable), glass windows with photomultiplier mounts (top right and bottom left), and PZT pin hydrophone ports with mounts (top right). Inlet and outlet fluid ports are located on top (shown with valve) and bottom. Liquid is pressurized using a 70 MPa (10 000 psi) high pressure generator (High Pressure Equipment, Erie, PA) attached to bottom of resonator. The calculated resonance frequencies of this device for the first five radially symmetric modes for D_2O at 20 °C are 9459, 13 314, 17 434, 24 131, and 30 993 Hz. For normal acetone at 20 °C they are 8226, 12 704, 14 938, 20 484, and 26 317 Hz (resonances near 13 000 Hz are associated with the SS shell motion). These values agreed fairly well with the measured ones. In both cases, the second mode corresponds to the resonance of the steel shell and closely reflected pressure release boundary conditions. For both liquids, the first frequency was lower and the third one was higher by a few percent compared to the calculated value using pure rigid boundary conditions. The effect of non-ideal rigid boundary condition on frequency above 20 kHz is less than 1%.

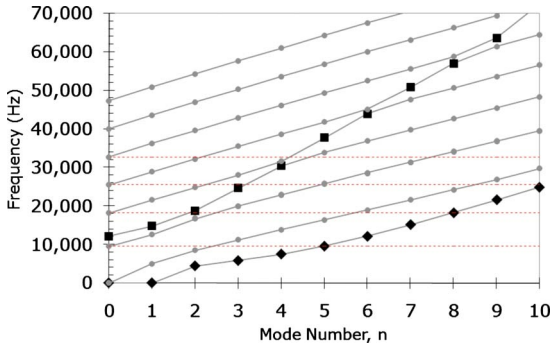

FIG. 2. (Color online) Mode structure of a 19 mm (3/4 in.) thick wall SS resonator filled with water using formulations given in Ref. 20. Symbols represent resonance frequencies while lines joining symbols are for visual aid. The lowest branch is the "bending" mode (diamond symbol), associated with bending effects in the shell. The "membrane" mode (dark squares), associated with stretching effects, can be seen cutting diagonally (from lower left to upper right) across the acoustic resonances starting with the $n=0$ shell mode at 12 787 Hz. For experiments, we use primarily the $n=0$ (acoustic) modes since they are the only ones with a pressure antinode at the center of the sphere. The first four acoustic modes are at 9,804, 18,290, 25,500, and 32,786 Hz, respectively. The horizontal lines at these values are visual aids for finding other nearby modes. Input parameters: H_2O density $=1{,}000\ \mathrm{kg/m^3}$, shell density$=7{,}800\ \mathrm{kg/m^3}$, Poisson ratio$=0.297$, H_2O sound speed$=1{,}483$ m/s, shell sound speed$=5{,}782$ m/s, and ratio of outer to inner shell radius$=1.1875$.

acoustic resonances of the liquid-filled sphere (we have investigated a number of liquids, including H_2O, D_2O, normal (NA) and deuterated (DA) acetone, and mixtures of acetone and water). In general, modes with frequencies in the range 20–50 kHz (exact values depend on liquid properties and resonator dimensions, see Fig. 2; formulation given in Ref. 20) were found to produce inertial transient cavitation requiring the least amount of electrical power, ranging between 1 and 250 W for static pressures between 0.1 and 30 MPa (1–300 bars). The observed resonance frequencies that are most efficient in generating cavitation are believed to be those near the main transducer resonance of 20 kHz.

Photomultiplier tubes (PMTs) and glass windows were used to measure the number of photons emitted from each SL pulse. Fast (Hamamatsu H6780 or R7400U, 0.75 ns rise time) PMTs were used to study the time dependence and the total number of photons. In the resonator, needle-type piezoelectric hydrophones (PZT pins, Dynasen Inc., Goleta, CA; http://www.dynasen.com/html/pinintro.html) in contact with the liquid (inserted through the steel shell) near the inner wall were used to measure the amplitude of the standing wave sound pressure as well as the pulses generated by the collapsing cavities. The sensing element in these hydrophones is a PZT disk, 1.25 mm diameter and 0.25 mm thick, with a rise time of ~ 35 ns. The PZT pins were calibrated in a test fixture using a Precision Acoustics (Dorchester, UK) 0.2 mm diameter polyvinylidene fluoride (PVDF) hydrophone (calibrated between 1 and 20 MHz) using fast (<35 ns) pressure pulses. A power amplifier (typically ENI 1140LA, 1500 W) and an impedance matching circuit (ENI EVB-1) were used to deliver the electrical power to the transducers. In addition, a high-speed camera (Imacon 200 by DRS Technologies (Parsipanny, NJ), 1360×1024 pixels) was used to image the cavitation events using 7 charge-coupled devices (CCD) (using each twice for a total of 14 frames) with maximum frame rate of 200 Mf/s. A still CCD camera was also used: Prosilica EC1390C, 1360×1024 pixels.

All data presented here were taken after extensive filtering (0.2 μm pore size) and degassing of the liquid, which was achieved by applying both a vacuum above the interface and heat to the bottom section of the resonator in order to enhance the nucleation of cavitation while sound was being applied. This nucleation process is an effective way to remove dissolved gases from liquids. The optimum degassing level, typically requiring a couple of hours to reach, was determined by the ability to achieve transient cavitation at high static pressures. This cavitation is usually accompanied by audible pinging sounds (shock waves from the cavitation collapse striking the walls of the resonator), and the absence of sustained broadband noise in the hydrophone trace—an indication of steady cavitation. When steady cavitation did occur, it was most commonly observed near the inner wall and/or in the fluid inlet and outlet ports of the resonator system.

III. OBSERVATIONS

A. Transient cavitation cavity/cluster/resonator dynamics

The resonator system has various time scales that affect the production of cavitation. An obvious time scale is the acoustic period of the driving frequency. A second one is the time for a shock wave, generated by a collapsing cavitation

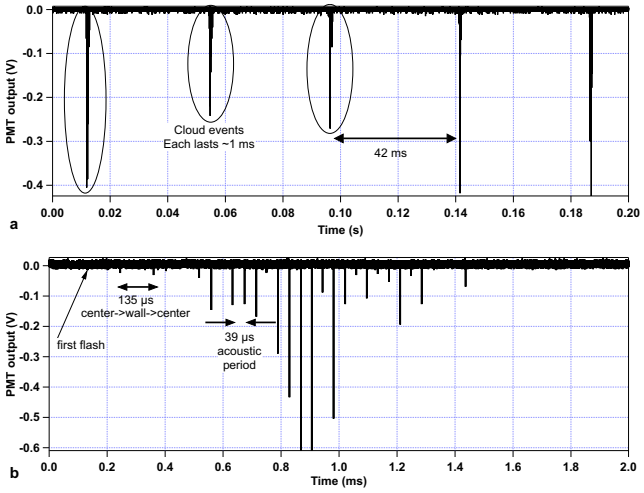

FIG. 3. (Color online) Timing diagrams for typical transient cavitation event in a high Q spherical resonator. (a) Each vertical line, about 42 ms apart, represents a cavitation event consisting of several light pulses generated by a cluster of collapsing bubbles. Each event lasts for about 1–2 ms, after which the bubbles dissolve back into the liquid. (b) Expansion in time of a cavitation event shown in (a). Here each vertical line represents a pulse of light, roughly one acoustic cycle apart ($\sim$39 μs). The first couple of pulses are probably due to the collapse of a single bubble right after nucleation. The initial increase, and subsequent decrease of the pulse amplitudes, can be explained by two different mechanisms working against each other: The increase is likely due to buildup of a cluster of bubbles, thus increasing the intensity of the collapses (Refs. 21 and 22); the decrease is likely due to the reduction in the sound field amplitude due to detuning of the resonator by the presence of the bubble cluster. The bubbles are believed to eventually (millisecond time scales) dissolve completely into the liquid as the sound amplitude decreases, allowing the sound field to build up again until the next cavitation event occurs. Experimental parameters: SS resonator ID: 203 mm, liquid H_2O, driving frequency $\sim$26 kHz, and static pressure $\sim$10 MPa.

bubble, to travel to the inside resonator wall, reflect, and return to the original site of cavitation. A third is associated with the detuning of the resonator due to cavitation-cluster buildup in the center of the sphere disturbing the otherwise resonant standing wave field. A fourth is the time it takes for the resonator to regain the pressure amplitude sufficient to generate another cavitation event. These time scales, with some specific numbers, are illustrated in Fig. 3.

Figure 3 illustrates the temporal behavior of SL emissions from the spherical resonator and thus describes the gross cavitation dynamics of this system. In Fig. 3(a), it is seen that the SL emissions appear to be repeated quite regularly, approximately every 42 ms. If this SL burst, which we believe is associated with the development of a cavitation "cloud" or "cluster," is expanded in time, there is a temporal structure to this burst that is in part characterized by the acoustic period of the sound field, viz., 39 μs. Also important, although not readily evident in this figure, is the time for a shock wave to travel to the wall, reflect, and return back to the center of the sphere—for this particular data set—135 μs (more on this later). Perhaps most obvious from this figure is the gradual increase, over a time period of about 1 ms, of the SL intensity to a maximum. After about 1 ms, there is a fairly rapid decrease of the SL intensity back to a minimum value. It should be noted that this increase in intensity is quite large, perhaps by a factor of nearly 100. Finally, before this sequence can be repeated, the resonator has to regain the original standing wave ratio that was necessary to initiate this sequence in the first place, a time period ranging between 20 and 200 ms (42 ms in this case, see Fig. 3), depending on electric power applied to the transducers. More power results in shorter recovery time.

From high-speed movies that we have made of this behavior, we believe that the following progression of events occurs: Because the acoustic rarefaction pressure is sufficiently in excess of the ambient pressure, a spontaneous cavitation event occurs. This bubble grows and collapses and generates daughter nuclei that survive until the next rarefaction cycle, which induces more bubbles to be nucleated and they in turn produce more daughter nuclei. This sequence continues, building up a cavitation cloud, or preferably, cavitation cluster, that is composed of many individual bubbles. Because the cluster is composed of several bubbles, the collapse of this cluster is more violent than the collapse of an individual bubble, and thus the SL intensity correspondingly increases.[21,22] (We also believe that the dynamics of a cluster collapse is even more violent than that for an individual bubble of comparable size.) When the cavitation cluster becomes sufficiently large, it scatters and absorbs so much acoustic energy that the resonator is rapidly detuned, the pressure amplitude drops below the threshold pressure, and cavitation ceases. The resonator gradually reestablishes the strong standing wave field and the sequence repeats. We have performed a series of experiments that show some remarkable details of the aforementioned behavior which is now described.

Recall that the ambient pressure in this resonator is quite large, say, 30 MPa (300 bars), and thus the cavitation collapses are quite violent; consequently, the shock waves produced are similarly quite intense—a topic that will be presented in a later publication. Because of the spherical symmetry of the resonator, and the fact that the best modes for producing cavitation are those with an antinode at the center of the resonator, the shock wave travels to the inner wall of the resonator, reflects, and converges on the cavitation cluster that still remains—note the time scales in Fig. 3. We wished to explore the possibility that this converging shock wave (with a positive pressure much larger than the resonator driving pressure) could implode a bubble or a cluster and generate a particularly violent collapse. However, because cavitation nucleation is basically a stochastic phenomenon, preventing temporal control over this behavior, we decided to use a laser to induce nucleation at a particular phase of the acoustic cycle and thus control, to a certain extent, the temporal dynamics of the entire event. (We also expect to report on this particular aspect of this study in a separate publication.) Here, we wish to show a few details of laser-induced nucleation, shock wave generation, and interaction between the shock wave and the bubble cluster. Experiments with fast neutrons (14.1 MeV) to trigger nucleation showed no obvious advantage over laser nucleation.

Shown in Fig. 4 is a series of photographs from a high-speed movie of a typical case of laser-induced nucleation and shock wave generation.

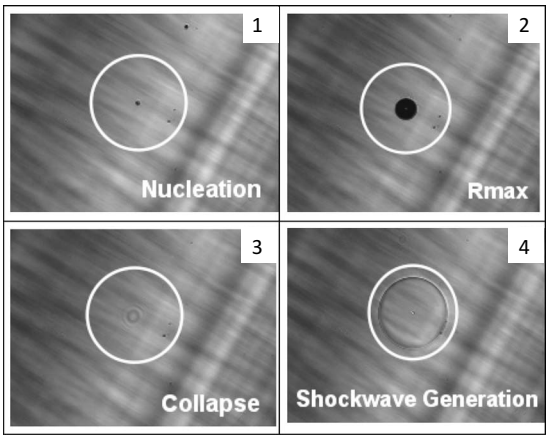

FIG. 4. Images of a cavitation event taken with the Prosilica EC1390C camera during the first acoustic cycle after nucleation triggered by a laser focused near the center of the resonator. The size of each frame is about 6.8×5.1 mm^2. The sequence is arranged chronologically from left to right, top to bottom, with an approximate frame-to-frame time of 12, 6, and 1 μs between images 1-2, 2-3, and 3-4, respectively, and with exposure times $\sim$20 ns. The white circles are for visual guidance. The maximum bubble radius in the second frame is about 1 mm. Shock velocities are slightly supersonic up to 1 mm or so. The image resolution does not allow for a determination of the minimum collapse radius (R_{min}). Experimental parameters: SS resonator ID: 203 mm, liquid H_2O, driving frequency $\sim$26 kHz, liquid temperature 24.0 °C, and static pressure 10 MPa.

It has been determined that this outgoing shock wave observed in Fig. 4 is quite intense and slightly supersonic during the first 1 mm of outward travel or so (more details in a subsequent paper). Computer simulations (unpublished, Ref. 23) indicate shock amplitudes on the order of 1–10 TPa (10–100 Mbars) shortly after its formation ($\leq$100 μm from the bubble wall), and Mach numbers around 10; accordingly, this shock has the ability to propagate to the inner wall of the resonator, reflect, and then converge onto the site at which it was generated, producing a violent implosion of the contents of the proceeding cavitation event that initially produced the shock.

We show in Fig. 5 some photographs taken with the Imacon high-speed camera that illustrates this very interesting phenomenon.

B. Pressure pulses

Figure 6(a) shows a sequence of pressure pulses detected by the PZT hydrophone located near the wall in the liquid in the SS resonator. Also shown in this figure are SL flashes. Both the acoustic pulses and SL flashes were generated by the collapse of cavities.

In Fig. 6(a), the acoustic pulse at time $\sim$110 μs is assumed to be due to the first collapse since no pulses are observed for several acoustic cycles before then. The SL associated with this acoustic pulse occurs at $\sim$40 μs. Note that the time interval between the first SL flash and pressure pulse ($\sim$70 μs) agrees with the time of flight of the pressure pulse from the center to the hydrophone located on the resonator wall. The first five pulses or so correspond to bubble or cluster collapses before any reflections have had time to reach the hydrophone, which should be around 135 μs (round trip from wall to center and back). In this case, the pulses are spaced $\sim 42 \pm 5$ μs apart corresponding to an acoustic cycle, the variation of ± 5 μs being likely caused by changes in the size of the emitting cavity and/or intercavity interactions. Eventually, the pressure signals become

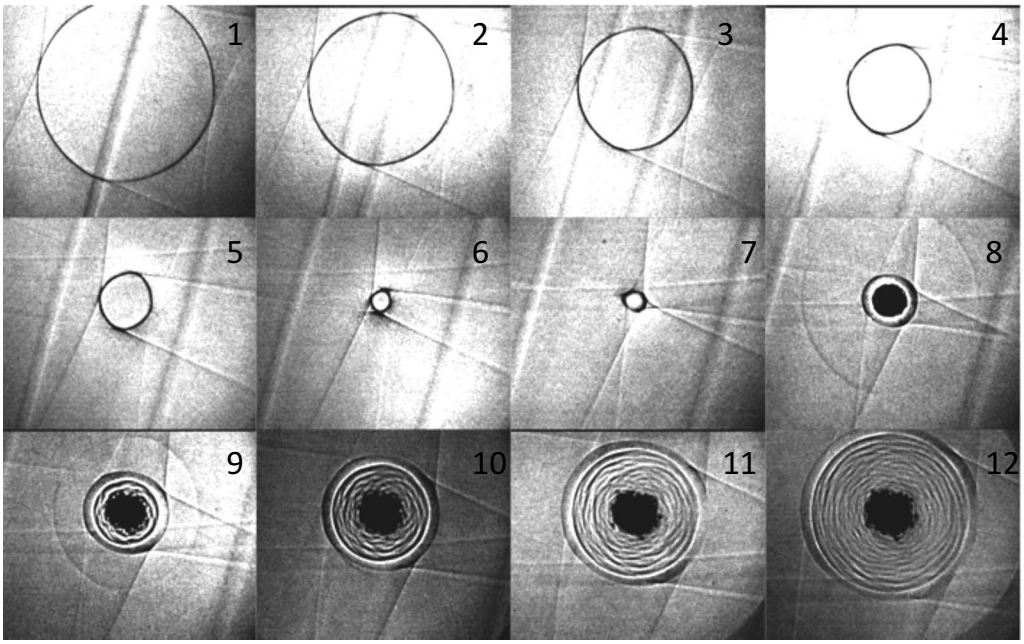

FIG. 5. Sequence of images taken with the Imacon 200 camera, about 500 ns apart with exposure time around 5 ns. The size of each frame is about 10×12 mm^2. The sequence is arranged chronologically from left to right, top to bottom, depicting the effect of the converging shock wave after having been reflected at the resonator wall. The shock wave will focus at the center if it originated there, but across from center relative to the point of origin otherwise. Consequently, the shock will sometimes focus at a point where there are no apparent pre-existing bubbles, as is the case here. The faint circles in images 8 and 9 surrounding the cavitation region are "ghosts" generated by the recycling of the seven CCDs in this camera. The patterns created after the wave reflects at the focus and rebounds are not completely understood. Experimental parameters: SS resonator ID: 203 mm, liquid H_2O, driving frequency $\sim$26 kHz, liquid temperature 24.0 °C, and static pressure 10 MPa.

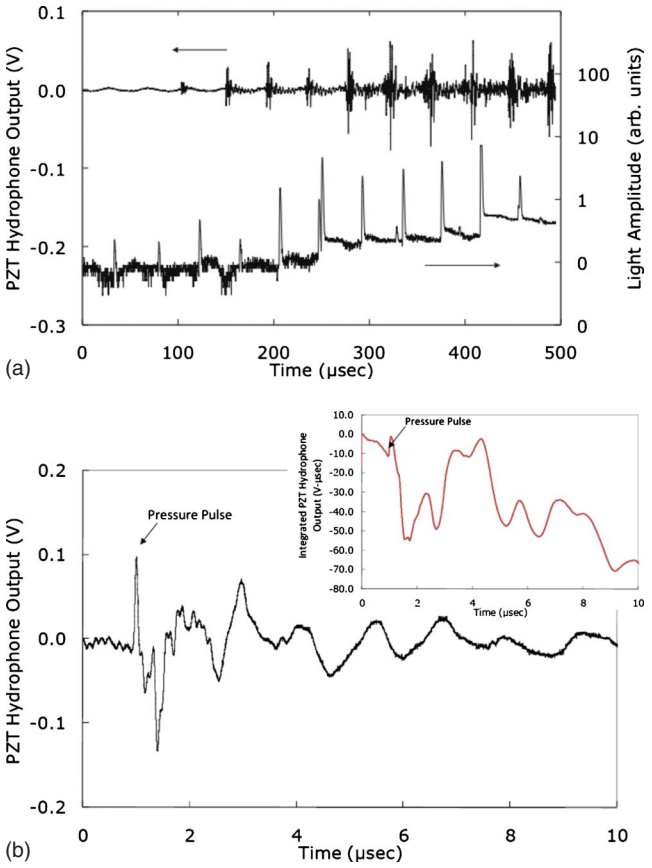

FIG. 6. (Color online) (a) Hydrophone (top) and photomultiplier tube (bottom) outputs for the first several acoustic cycles following a typical nucleation event in the spherical resonator. Most often, one collapse per cycle was observed, as can be seen in both the light and acoustic emissions. Note the log scale on the PMT output. The shift in the baseline of the bottom plot is an electronic artifact due to the high repetition rate of the signal. On the average, both the acoustic and SL emissions become stronger as the bubble cluster develops, as illustrated in this particular data set. Experimental parameters: SS resonator ID: 203 mm, liquid D_2O, acoustic pressure ~9.0 MPa (90 bars), driving frequency ~24 200 Hz, liquid temperature 24.0 °C, and static pressure 5.5 MPa (55 bars). (b) Oscilloscope trace of the PZT hydrophone response to a pressure pulse generated by cavitation collapse. The transducer is located on the inside wall of the spherical resonator and terminated in 50 Ω (see text for transducer details). On this time scale, the voltage is proportional to the time derivative of the acoustic pressure (the integrated voltage signal is shown in the small inset graph for reference). The amplitude of the first peak for transducers similar to this one was calibrated against the Precision Acoustics PVDF hydrophone, giving a rough calibration of 100 mV/MPa. The ~1 and ~10 MHz ringing are attributed to the radial and thickness resonance frequencies of the PZT element, respectively. The arrows point to the pressure pulse in each of the graphs.

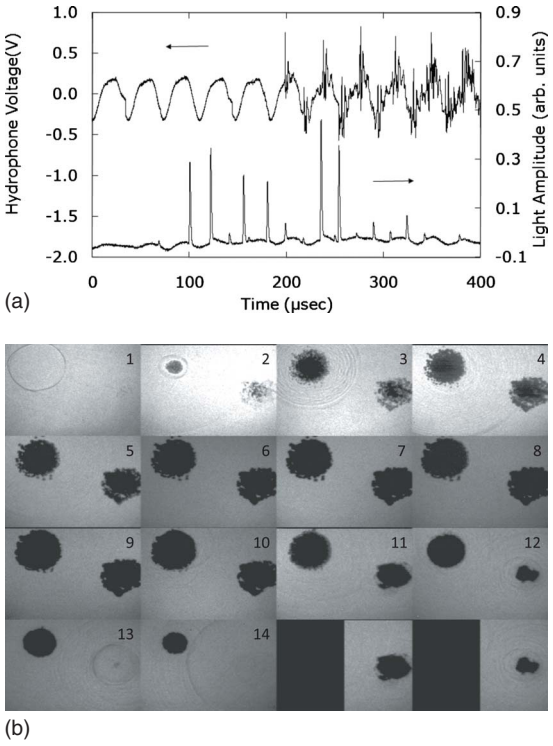

FIG. 7. (Color online) (a) PZT hydrophone and PMT outputs for the first several acoustic cycles of a cavitation event in which two pressure pulses and two SL flashes per cycle were observed. Pressure pulses and SL flashes are generated by the collapse of cavities in the liquid. It is likely that this result is due to the presence of two clusters which collapse at different times, as shown in (b). Experimental parameters: SS resonator ID: 216 mm, liquid D_2O, acoustic pressure ~150% of threshold value at given P_{stat}, driving frequency ~27 200 Hz, liquid temperature 17 °C, and static pressure 4.8 MPa. (b) Sequence of images taken with the Imacon 200 camera, about 2 μs apart with exposure time around 5–20 ns. The size of each frame is about 6×10 mm^2. The sequence is arranged chronologically from left to right, top to bottom, depicting the dynamics of two clusters in the same pressure antinode. The geometric center of the resonator where the pressure antinode is located is near the center on the images in this figure. In frame 1, a converging shock wave can be seen (top-left) which was (probably) previously created 135 μs earlier (see Fig. 3) by the cluster on the bottom-right, more clearly seen starting in frame 2. This shock wave converges and reflects at its focus between frames 1 and 2. The reflected shock (now moving outward in frame 2) nucleates a cluster. Both clusters expand during the negative acoustic half-cycle (approximately frames 1–8), although the pre-existing cluster on the bottom-right collapses several microseconds earlier compared to the cluster on the top-left, resulting in two SL pulses in one acoustic cycle (occasionally observed by naked eye or camera). Experimental parameters: SS resonator ID: 203 mm, liquid H_2O, driving frequency ~26 kHz, liquid temperature 24.0 °C, and static pressure 10 MPa.

less clear due to the superposition of direct and reflected pulses. The pulses should consist of a positive pressure wave followed by a smaller negative wave as expected from a spherically diverging wave.[24] The observed rise time of ~35 ns [Fig. 6(b)] is most likely dominated by the response time of the PZT hydrophone. The original pressure wave generated at stagnation is probably supersonic with rise time on the order of 1 ns (Refs. 25 and 26) although attenuation and acoustic dispersion during the 10 cm transit distance in the liquid is expected to increase the rise time of the measured pulse.[27]

The observation of one pressure pulse every cycle shown in Fig. 6(a) is the norm. However, in some cases, two SL flashes and two acoustic pulses [Fig. 7(a)] per cycle have been observed. Although non-linear bubble dynamics simulations do show supraharmonic motion where two or more R_{min} occur per cycle, usually only one of them results in pressures and temperatures large enough to emit SL, and thus it is not a likely explanation for this observation. A possible explanation is that simultaneous bubble clusters have formed in adjacent antinodes, which has been visually observed occasionally, and would result in the two clusters being driven with phases 180° apart. Because it is desirable to work with spherically symmetric modes ($n=0$) that have a single antinode at the center for easier interpretation of the results,

situations such as that shown in Fig. 7(a) are avoided. Finally, a more likely explanation is the presence of two simultaneous nucleation sites as observed with imaging devices [e.g., Imacon 200 camera and shown in Fig. 7(b)] or even with the naked eye above ~100 bars (where the SL intensity is high enough).

The two SL sites are opposite each other relative to the sphere center, and are created when the collapse of one cavitation event [bottom-right in images in Fig. 7(b)] generates a shock wave that is reflected and focused by the resonator wall back toward the center [top-left in frame 1, Fig. 7(b)], triggering a new cavitation site. It can be shown using simple geometry that a spherical wave generated slightly off center and reflected by a spherical boundary will be focused in a region equidistant from the center but opposite to the original source. For a rigid wall, the timing is such that it takes an odd number of half-cycles for the shock wave to return to the center. Since the original shock is normally created at the end of a bubble or cluster collapse when the acoustic pressure is positive, the shock wave converges near its point of origin during the negative acoustic half-cycle. This appears to be the case for a rigid-wall resonator regardless of the resonance mode being used. Thus, the acoustic pressure is negative in frames 2–11 and positive in the others, consistent with the cluster on the right expanding in frames 2–8, and starting to collapse in frame 9, reaching R_{min} between frames 12 and 13, where a SL pulse should be emitted. The cluster on the left is also collapsing and should reach R_{min} in two to three frames (4–6 μs), judging by the collapse time of the cluster on the right. Thus, this situation leads to two SL pulses per cycle and could explain Fig. 7(a).

In an effort to study the effect of bubble cluster formation, we have examined pressure pulses as a function of the temporal position in the evolution of the bubble cluster. In Fig. 8, the amplitude of pressure pulses has been plotted vs P_{stat} for the first (asterisks) and the largest (solid squares) pulses for individual cavitation events. The fact that the largest pulses occur in the middle of the cavitation-cluster event [see Fig. 3(b)] suggests that the presence of the cluster is increasing the strength of the collapses. For these data, the PZT transducer was calibrated using the PVDF hydrophone calibrated between 1 and 20 MHz. These values should be viewed with caution, however, since it is not known at this point how much energy of the pulse might be above 20 MHz.

C. Light pulses (SL)

Similar to pressure pulses, light flashes or pulses are observed corresponding to the pressure pulses for the first several cycles after cavitation inception, as shown in Fig. 9. The main difference, however, is that the number and intensity of the SL flashes depend strongly on P_{stat}. At low pressures (<0.1 MPa), few, small flashes are observed only during the first couple of cycles, with the number and amplitude of the flashes increasing as the static pressure is increased. Furthermore, similar to the pressure pulses, the largest SL flashes occur later in the cavitation event after the bubble cluster has formed. Again, this suggests that the cluster enhances the strength of the collapse.

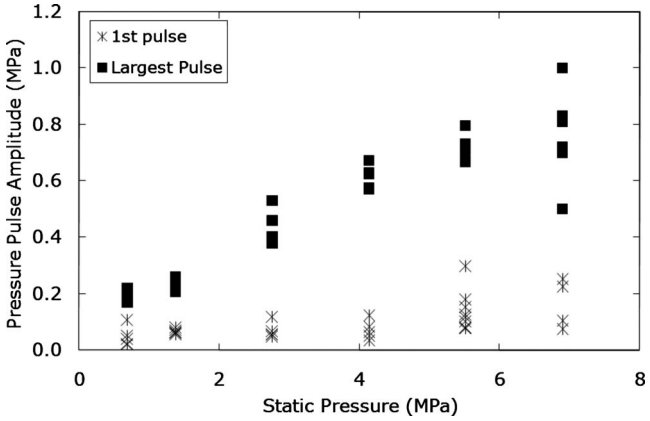

FIG. 8. Amplitude of pressure pulses measured by a PZT hydrophone in the liquid close to the SS spherical resonator wall (≤1 mm), and about 102 mm from the center where the cavitation occurred. The largest pulses (square symbols) typically occurred between 5 and 20 acoustic cycles after nucleation and were on the average larger than the first pulse (asterisks) in the cavitation event. These data seem to indicate that collapses generated by the cavitation cluster are more violent than the first collapse, assumed to be from a single cavity (see text, Fig. 3). Experimental parameters: SS resonator ID: 203 mm, liquid D_2O, acoustic pressure ~150% of threshold value at given P_{stat}, driving frequency ~24 300 Hz, and liquid temperature 24 °C. The calibration was performed with a Precision Acoustics 0.2 mm diameter PVDF needle hydrophone calibrated in the range 1–20 MHz.

In an attempt to evaluate the effect of static pressure, the light emission was investigated near the cavitation threshold at increasing static pressures ranging from <0.1 MPa (<1 bar) to 14.0 MPa (140 bars). Figure 10 shows the pulse height (approximately number of photons) distribution for three values of the static pressure for D_2O, clearly indicating that the light pulses are becoming both larger in amplitude

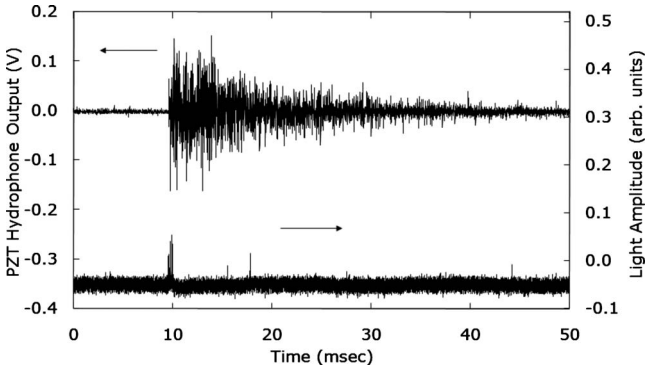

FIG. 9. Acoustic (top) and light (bottom) emissions of a typical cavitation event. The hydrophone signal measured with the PZT transducer is terminated. The hydrophone signal is terminated in 50 Ω (creating an effective high-pass *RC* filter) so the 24 kHz driving acoustic signal is filtered and only the high frequency acoustic emissions are recorded. Note that most of the light emission occurs within the first couple of cycles of the cavitation event while the bubble cluster is present and active. In the resonator, the lifespan of the high frequency emissions ranged between 10 and 50 ms depending on the acoustic mode, and the number of light flashes per event ranged between 1 and 50 (due to the time scale shown in this figure, there are several individual SL flashes within the spikes shown in the lower trace; see Fig. 3). The long duration of the acoustic emissions (greater than bubble cluster duration) is assumed to be the result of the low dissipation in the system. Experimental parameters: SS resonator ID: 216 mm, liquid D_2O, acoustic pressure ~4.0 MPa, driving frequency 27 211 Hz, liquid temperature +17 °C, and static pressure 0.7 MPa.

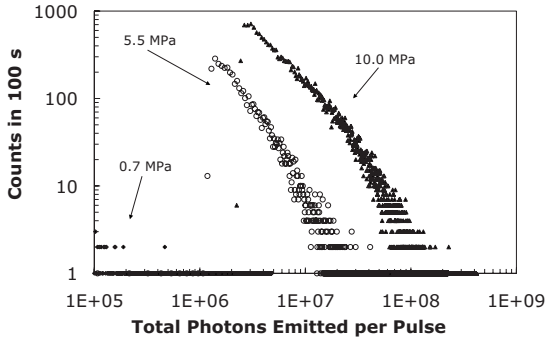

FIG. 10. Pulse height distribution of sonoluminescence flashes (pulses) illustrating the increase in both the number of pulses/s and the amplitude (number of photons/pulse) as the pressure is increased. The vertical axis is the total number of pulses in 100 s in a given range (bin width) of photons/pulse. Bin width is 2,300, 110,000, and 200,000 photons for 0.7, 5.5, and 10 MPa respectively. The number of photons has not been adjusted for the quantum efficiency of the PMT. The data were taken at acoustic pressures just above the cavitation threshold. Experimental parameters: SS resonator ID: 203 mm, liquid D_2O, acoustic pressure ~150% of threshold value, driving frequency ~24 100 Hz, and liquid temperature 16 °C.

and more numerous (per unit time) as the static pressure is increased. Note that the number of photons emitted by a typical SBSL flash in water is on the order of 10^5, three orders of magnitude fewer than the largest pulse shown in Fig. 10.

Since the nucleation rate was kept approximately constant, the data also indicate that the number of flashes per cavitation event increases with P_{stat}. Similar results were observed for other liquids. The amplitude of the larger pulses vs P_{stat} has been plotted for three different liquids in Fig. 11.

These data also show that the number of photons increases approximately linearly with the static pressure, although some degree of saturation is observed due to extraneous cavitation at the higher pressure values. The maximum P_{stat} at which transient cavitation was possible as well as the intensity of the SL flashes could vary greatly depending on

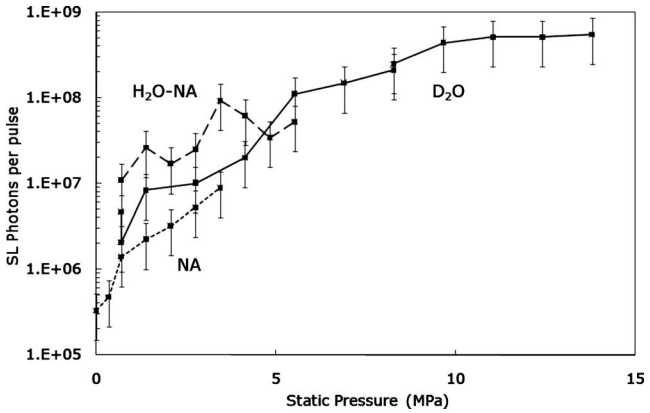

FIG. 11. Number of photons per flash vs static pressure in the SS spherical device. The number of photons plotted are for the brightest flashes observed at each value of the static pressure. The number of photons has not been adjusted for the efficiency of the PMT. Experimental parameters: SS resonator ID: 216 mm, dashed Line: 50% normal acetone (NA)/50% H_2O mixture, 28.5 kHz, 23.2 °C, voltage to transducer was kept constant at 350 Vrms, dotted Line: normal acetone, 26.9 kHz, −4.0 °C, voltage to transducer was kept constant at 350 Vrms, solid Line: D_2O, 28.6 kHz, 21.0 °C, and acoustic pressure ~150% relative to cavitation threshold.

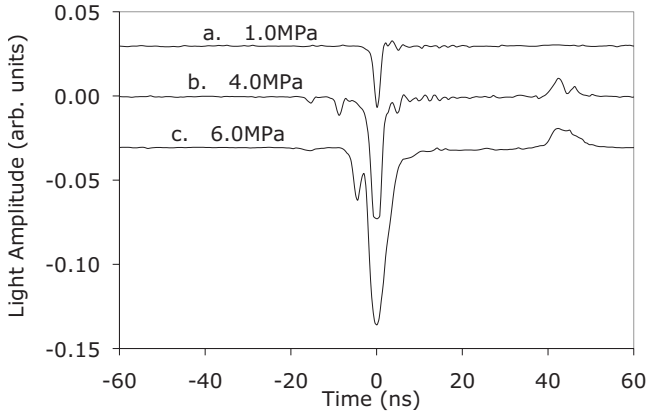

FIG. 12. Typical shapes of light flashes measured with a fast photomultiplier tube (<1.0 ns rise time) in D_2O as the static pressure was increased. These data illustrate how the light flashes increase both in amplitude and width with the static pressure. In addition, earlier flashes in the cavitation event were more uniform (fewer peaks) and occasionally brighter compared to later ones in the same event. The less uniform flashes (more peaks) could be the result of bubble-bubble interaction and/or multiple SL flashes from different cavities within the cavitation cluster. Experimental parameters: liquid D_2O, acoustic pressure ~150% of threshold value for given P_{stat}, driving frequency ~28 500 Hz, liquid temperature 23.2 °C, and static pressure ranged from (a) 1.0, (b) 4.0, and (c) 6.0 MPa.

how well the liquid was degassed and/or the particular mode being driven. The increase in light emission vs P_{stat} is not surprising since the acoustic pressure driving the collapse must also be increased in order to reach the cavitation threshold—where the threshold is defined as the negative absolute pressure necessary to expand the initial cavity to macroscopic size. The saturation effect could also be an indication of instabilities during the collapse, although more data will be required before making a determination.

We have also examined the SL pulse shape as a function of static pressure; these data are shown in Fig. 12. In general, both the pulse width and amplitude increase with P_{stat} suggesting that the collapse intensities are increasing with P_{stat}.

The larger amplitudes are consistent with higher plasma temperatures and/or larger bubbles (more gas or vapor inside cavities). The variation in the intensity of the light flashes (multiple peaks per flash) is also consistent with higher energy densities in the gas phase, particularly if any of the peaks are caused by shock waves during the final stages of the collapse, as computer simulations have suggested.[28] It should be noted, however, that these peaks could also be the results of multiple, independent cavities collapsing very near to each other, judging by the short time difference between peaks (on the order of nanoseconds).

IV. DISCUSSION

Transient acoustic cavitation in highly pressurized liquids is a particularly effective way to generate extremely energetic phenomena. In the time interval between cavitation events, the acoustic energy is able to build up to large values in the absence of any inhomogeneities in the liquid (e.g., cavities or bubbles) that disturb the resonance. Thus, when a cavity forms spontaneously, it is greatly expanded, absorbing large amounts of acoustic energy. This energy is converted to potential energy when the liquid pressure becomes positive

again in the following acoustic half-cycle. This process creates an out-of-equilibrium situation with a nearly empty cavity surrounded by a high pressure liquid, resulting in the rapid collapse of the cavity. During this collapse, work is done on the small amount of gas or vapor in the cavity and it is thus compressed and heated. The initial acoustic energy of the liquid is converted to thermal energy in the gas via the cavitation process. Thus acoustic cavitation converts and focuses energy from the initial, relatively low, acoustic energy density to the resulting high-energy-density "hot spot" at stagnation.

Transient cavitation in the resonators described here is particularly intense because it occurs at very high static and acoustic pressures, resulting in a larger pressure differential between the liquid and bubble interior and, consequently, higher speeds of collapse. Furthermore, due to the high degree of relative degassing, few bubbles ($\sim$1–20) are present at any one time, increasing the expansion of each bubble[29] and therefore the collapse energy.

Evidence of this increase in intensity can be found in Fig. 4 where images of shock waves emitted at the end of the bubble collapse are shown. Judging by the high contrast of these images in comparison with those of SBSL shock waves,[30] the shock amplitudes appear to be significantly larger, although quantitative comparison is not possible at this time due to experimental constraints. Theoretical estimates based on numerical hydrocodes,[31] however, give shock amplitudes in the range 1–10 TPa (10–100 Mbars, compared to 100 kbars for SBSL).

The shock waves reflected at the inner resonator wall will re-focus at the center, as long as it originated there (otherwise, the focus is across the center from its place of origin). These converging waves also generate very intense phenomena judging by the high-contrast images and their ability to cavitate the liquid [see last five images in Figs. 5 and 7(b)]. The images show a well-defined shock front in the converging waves (thin black circles in first six images in Fig. 5). The reflected, diverging waves have more structure; however, a double shock front with random waves inside them as well as a dark region in the center is apparently due to bubbles or cavities nucleated by the wave. We have no clear explanation for these double-front shock waves yet. Unfortunately, our current resonators were not designed with this reflecting shock front in mind, and thus the reflected, converging shock waves do not arrive at the focus at a particularly propitious point in the cavitation cycle. For example, if it were to arrive at a time when a bubble cluster was just starting to collapse, extremely violent cavitation collapse may well occur.

Degassing the liquid was often observed to reduce the "hissing" noise generally associated with cavitation at or near the resonator walls. Nevertheless, violent, transient cavitation was still possible at high P_{stat} as long as the amount of dissolved gas remained constant, indicating that the gas concentration relative to saturation (at a given P_{stat}) is the relevant parameter controlling this type of cavitation. At large relative gas concentrations (e.g., low P_{stat} using H_2O saturated at ambient conditions) steady cavitation was observed for electric power levels comparable to those used during transient cavitation. Steady cavitation (evidenced by the continuous presence of a cluster of bubbles at the center of the resonator) degrades the quality factor such that intense cavitation and associated shock waves are not generated.

Typical measured Q values were in the range 10 000–200 000, even for (apparently) identical resonators, the cause of the large variation not being currently understood. For comparison, theoretical Q values using classical damping mechanisms (bulk thermal conduction and viscosity plus thermal conduction at the wall) are around 1.5×10^6 for the 25 kHz mode, about ten times larger than measured. A different model using complex elastic modulus in solids[32] to include losses in the SS shell and using the measured Q of the empty shell ($\sim$10 000) gives Q values of $\sim0.8\times10^6$ (3.9×10^6 for $Q_{shell}=20\,000$). Clearly, the dominant acoustic loss mechanism is yet to be determined and even higher Q resonators might be possible.

Although there is an infinite number of resonance modes for a liquid-filled sphere (even for only the spherical modes, $n=0$), we are able to achieve intense transient cavitation only for a few modes. The requirement that cavitation be near the center (i.e., well localized for imaging and diagnostics) means that only the spherical modes ($n=0$) are to be used. Furthermore, since large Q values were required, only frequencies below $\sim$50 kHz or so are available. In general, low Q values are observed above that frequency, apparently due to interference (overlapping) between adjacent modes at the higher frequencies (mode density increases dramatically with frequency). Typically, for the $n=0$ modes, Q values greater than 10 000 were observed only for the 25, 33, and 42 kHz modes (see Fig. 2) in the 241 mm OD (9.5 in OD) spherical resonators (the 10, 12, and 18 kHz modes had Qs less than 5000). Smaller resonators have significantly lower Q values.

V. CONCLUSIONS

Transient cavitation in highly degassed and cleaned liquids consists of expansion and collapse of a single cavity followed by the formation of a cluster within a few acoustic cycles ($\sim$100 μs after nucleation). The presence of the cavity cluster detunes the resonator and dissipates acoustic energy, causing the sound amplitude to decrease and the bubbles to disappear within a few milliseconds. The fact that the cluster disappears indicates that the cavities are filled with mostly vapor, which condenses readily in the absence of the sound field. The duration of the cluster remains fairly constant (2 ± 1 ms) for pressures above 0.1 MPa, increasing rapidly for pressures below this value to about 15 ± 5 ms. How long the resonator remains detuned, however, depends on the persistence time of the acoustic waves in the liquid which should be directly proportional to the Q factor and inversely proportional to the power applied to the acoustic drivers. We observed persistence times in the resonators of about 20-200 ms.

Light pulses and shock waves were observed simultaneously with bubble collapse. The amplitudes of both light pulses and shock waves increased as a function of static pressure at acoustic pressures near the threshold for cavitation. The amplitude of both the light pulses and the shock waves

were about 1000× larger compared to SBSL values (10^9 photons/pulse and 1–10 TPa). These shock waves were observed to reflect off the inner resonator wall and re-focus near the center, the exact position depending on their place of origin. Since the reflected waves were strong enough to trigger cavitation, we therefore conclude that they represent a new mechanism for generating extreme conditions using cavitation in liquids.

The amplitude and width of the light pulses increased with the static pressure. The wider pulses (>5 ns) associated with collapses above ~3.0 MPa have features that are not smooth, which could be caused by multiple flashes from individual bubbles collapsing very close to each other. Alternatively, one (or some) of these features that occur prior to the peak light emission might be the result of multiple incandescent shock waves generated during the collapse inside or outside the cavities. Computer simulations indicate that the shock formed near the bubble is able to heat the liquid sufficiently to emit photons for several nanoseconds. More accurate computer simulations of single cavities might help elucidate the gas dynamics responsible for the observed features in the light pulses.

Light pulses and shock waves were observed with repetition frequencies of half, equal, and twice the acoustic frequency. Normally one would expect one collapse per cycle based on single and multi-bubble SL observations, although highly non-linear motion of a bubble or cluster has been known to exhibit complex subharmonic and supraharmonic motion.[33] Double SL and pressure pulses per cycle can be explained by either two cavitation regions in adjacent antinodes or in the same antinode but having different collapse times.

We did not observe significant difference in the light emission from the liquids investigated (normal and deuterated acetone, water, heavy water, and mixtures thereof), at equivalent high operational static pressures. In SBSL, which is normally measured in low Q resonators near 0.1 MPa (1 bar), acetone (and other non-aqueous liquids) typically produces at least two orders of magnitude fewer photons per pulse compared to water[5,34] and similar figures for SL pulses per acoustic cycle. Note that SBSL in water generates one SL pulse every cycle. Furthermore, the SL output from transient cavitation in our resonators (both photons/pulse and pulses/s) is orders of magnitude lower at low P_{stat} (a few bars) compared to high pressures (>50 bars; see Fig. 10). The dramatic difference in SL output in the two pressure regimes and the insensitivity to the liquid suggests that transient cavitation at high static pressures is qualitatively a different phenomenon compared to SBSL, perhaps due to the lack of diffusion equilibrium between liquid and the bubble interior. In addition, it appears that in order to enable cavitation at high static pressure, it is necessary to construct a resonator with a high Q factor.

We also investigated transient cavitation triggered three different ways: (1) fast (14.1 MeV) neutrons impinging on the liquid, (2) focused high intensity lasers, and (3) spontaneous cavitation presumably on gas pockets on dirt particles. No significant difference was observed among these three types of cavitation in terms of light or acoustic emissions.

These studies demonstrate that extremely violent cavitation events can be generated by our high Q, spherical resonator system that can generate cavitation at relatively large ambient pressures. We believe that we have generated the most intense cavitation ever observed, much of which we do not understand. We note that we do not observe significant saturation behavior in the shock wave amplitudes as P_{stat} is increased (Fig. 8), indicating that the upper limit of cavitation intensity has not yet been reached. We expect to report on a number of additional results in the immediate future, particularly that of generating cavitation in liquid metals and other exotic transparent media, in which much more violent cavitation is expected over that in water and other low-density fluids.

ACKNOWLEDGMENT

We are grateful to J. Mobley, J. Lonzaga, and W. Prather at the National Center for Physical Acoustics (University of Mississippi) T. Murray, P. Anderson and J. Sukovich at the Boston University, and D. Giraud and B. MacConaghy at the University of Washington for measurements on the resonators. This work was supported in part by the Space Missile and Defense Command (SMDC) under Contract No. W9113M-07-C-0178.

[1] B. P. Barber and S. J. Putterman, "Observation of synchronous picosecond sonoluminescence," Nature (London) **352**, 318–320 (1991).
[2] W. C. Moss and D. A. Young, "Calculated pulse widths and spectra of a single sonoluminescence bubble," Science **276**, 1398–1401 (1997).
[3] A. Bass, S. J. Ruuth, C. G. Camara, B. Merriman, and S. J. Putterman, "Molecular dynamics of extreme segregation in a rapidly collapsing bubble," Phys. Rev. Lett. **101**, 234301 (2008).
[4] D. Shapira and M. Saltmarsh, "Nuclear fusion in collapsing bubbles—Is it there? An attempt to repeat the observation of nuclear emissions from sonoluminescence," Phys. Rev. Lett. **89**, 104302 (2002).
[5] C. G. Camara, S. D. Hopkins, K. S. Suslick, and S. J. Putterman, "Upper bound for neutron emission from sonoluminescing bubbles in deuterated acetone," Phys. Rev. Lett. **98**, 064301 (2007).
[6] R. Geisler, W. D. Schmidt, T. Kurz, and W. Lauterborn, "Search for neutron emission from sonoluminescing in laser induced cavitation," Europhys. Lett. **66**, 435–440 (2004).
[7] W. C. Moss, D. A. Young, J. A. Harte, J. L. Levatin, B. F. Rozsnyai, G. B. Zimmerman, and I. H. Zimmerman, "Computed optical emissions from a sonoluminescing bubble," Phys. Rev. E **59**, 2986–2992 (1999).
[8] W. B. McNamara III, Y. T. Didenko, and K. S. Suslick, "Sonoluminescence temperatures during multi-bubble cavitation," Nature (London) **401**, 368–371 (1999).
[9] S. J. Putterman and K. R. Weninger, "Sonoluminescence: How bubbles turn sound into light," Annu. Rev. Fluid Mech. **32**, 445–476 (2000).
[10] D. J. Flannigan, S. D. Hopkins, C. G. Camara, S. J. Putterman, and K. S. Suslick, "Measurement of pressure and density inside a single sonoluminescing bubble," Phys. Rev. Lett. **96**, 204301 (2006).
[11] Y. T. Didenko, W. B. McNamara III, and K. S. Suslick, "Temperature of multibubble sonoluminescence in water," J. Phys. Chem. A **103**, 10783–10788 (1999).
[12] W. B. McNamara III, Y. T. Didenko, and K. S. Suslick, "Pressure during sonoluminescence," J. Phys. Chem. B **107**, 7303–7306 (2003).
[13] D. J. Flannigan and K. S. Suslick, "Plasma formation and temperature measurement during single-bubble cavitation," Nature (London) **434**, 52–55 (2005).
[14] C. G. Camara, S. J. Putterman, and E. Kirilov, "Sonoluminescence from a single bubble driven at 1 Megahertz," Phys. Rev. Lett. **92**, 124301 (2004).
[15] D. F. Gaitan, Ph.D. thesis, University of Mississippi, MS, 1989 (available on-line through Dissertation Express, http://disexpress.umi.com/dxweb); D. F. Gaitan, L. A. Crum, C. C. Church, and R. A. Roy, "Sonoluminescence and bubble dynamics for a single, stable cavitation bubble," J. Acoust. Soc. Am. **91**, 3166–3183 (1992).

[16]D. F. Gaitan, "Sonoluminescence and bubble stability," Phys. World **12**, 20–21 (1999).
[17]D. F. Gaitan and L. A. Crum, "Observations of sonoluminescence from a single, stable cavitation bubble in a water/glycerin mixture," from the *Proceedings of the 12th International Symposium on Nonlinear Acoustics*, edited by M. F. Hamilton and D. T. Blackstock (Elsevier Science, New York, 1990), pp. 459.
[18]L. A. Crum, "Sonoluminescence," Phys. Today **47**(9), 22–29 (1994).
[19]S. J. Putterman, "Sonoluminescence: Sound into light," Sci. Am. **272**(2), 46–51 (1995).
[20]J. Mehl, "Spherical acoustic resonator: Effects of shell motion," J. Acoust. Soc. Am. **78**, 782–788 (1985).
[21]I. Hansson and K. A. Mørch, "The dynamics of cavity clusters in ultrasonic (vibratory) cavitation erosion," J. Appl. Phys. **51**, 4651–4658 (1980).
[22]C. E. Brennen, *Cavitation and Bubble Dynamics* (Oxford University Press, Oxford, 1995), pp. 158.
[23]D. F. Gaitan, R. A. Hiller, and R. A. Tessien, "Computer simulations of cavitation collapses at high static pressure: Plasma conditions and shock waves in the liquid," 18th International Symposium on Nonlinear Acoustics, Stockholm, Sweden (2008).
[24]Y. B. Zeldovich and Y. P. Raizer, *Physics of Shock Waves and High-Temperature, Hydrodynamic Phenomena* (Academic, New York, 1967), Vol. **1**, pp. 14.
[25]D. T. Blackstock, "Physical properties and behavior of shock waves," J. Acoust. Soc. Am. **114**, 2453 (2003).
[26]W. Eisenmenger, "Experimentelle Bestimmung der Stobfrontdicke aus dem akustischen frequenzspektrum elektromagnetisch erzeugter Stobwellen in Flüssigkeiten bei einem Stobdruckbereich von 10 atm bias 100 atm (Experimental determination of the shock front thickness from the acoustic frequency spectrum of electromagnetic generated shockwaves in fluids at pressures from 10 to 100 atm)," Acustica **14**, 187–204 (1964).
[27]A. D. Pierce, *Acoustics* (AIP, New York, 1989), pp. 590.
[28]R. Hiller and D. F. Gaitan, "Optical measurements of the hot spot and incandescent shock from high-pressure cavitation in water (A)," J. Acoust. Soc. Am. **123**, 3559 (2008).
[29]Preliminary computer simulations of acoustically driven bubble clusters indicate bubble expansion is inhibited when bubbles are too close to each other.
[30]J. Holzfuss, M. Rüggeberg, and A. Billo, "Shock wave emissions of a sonoluminescing bubble," Phys. Rev. Lett. **81**, 5434–5437 (1998).
[31]T. J. Larsen and S. M. Lane, "HYADES — A plasma hydrodynamics code for dense plasma studies," J. Quant. Spectrosc. Radiat. Transf. **51**, 179-186 (1994).
[32]A. D. Pierce, *Acoustics* (AIP, New York, 1989), pp. 145.
[33]R. G. Holt, D. F. Gaitan, A. A. Atchley, and J. Holzfuss, "Chaotic Sonoluminescence," Phys. Rev. Lett. **72**, 1376–1379 (1994).
[34]K. Weninger, R. A. Hiller, B. P. Barber, D. Lacoste, and S. J. Putterman, "Sonoluminescence from single bubbles in non-aqueous liquids: New parameter space for sonochemistry," J. Phys. Chem. **99**, 14195–14197 (1995).